



Mitigating the impact of dense vegetation on the Sentinel-1 surface soil moisture retrievals over Europe

Samuel Massart, Mariette Vreugdenhil, Bernhard Bauer-Marschallinger, Claudio Navacchi, Bernhard Raml & Wolfgang Wagner

To cite this article: Samuel Massart, Mariette Vreugdenhil, Bernhard Bauer-Marschallinger, Claudio Navacchi, Bernhard Raml & Wolfgang Wagner (2024) Mitigating the impact of dense vegetation on the Sentinel-1 surface soil moisture retrievals over Europe, European Journal of Remote Sensing, 57:1, 2300985, DOI: [10.1080/22797254.2023.2300985](https://doi.org/10.1080/22797254.2023.2300985)

To link to this article: <https://doi.org/10.1080/22797254.2023.2300985>



© 2024 The Author(s). Published by Informa UK Limited, trading as Taylor & Francis Group.



Published online: 10 Jan 2024.



Submit your article to this journal [↗](#)



Article views: 458




View related articles [↗](#)



View Crossmark data [↗](#)

Mitigating the impact of dense vegetation on the Sentinel-1 surface soil moisture retrievals over Europe

Samuel Massart¹^a, Mariette Vreugdenhil^a, Bernhard Bauer-Marschallinger^a, Claudio Navacchi^a, Bernhard Raml^a and Wolfgang Wagner^{a,b}

^aDepartment of Geodesy and Geoinformation, Vienna University of Technology, Vienna, Austria; ^bEODC Earth Observation Data Centre for Water Resources Monitoring, Vienna, Austria

ABSTRACT

The C-band Synthetic Aperture Radar (SAR) on board of the Sentinel-1 satellites have a strong potential to retrieve Surface Soil Moisture (SSM). Using a change detection model to Sentinel-1 backscatter, an SSM product at a kilometre scale resolution over Europe could be established in the Copernicus Global Land Service (CGLS). Over areas with dense vegetation and high biomass. The geometry and water content influence the seasonality of the backscatter dynamics and hamper the SSM retrieval quality from Sentinel-1. This study demonstrates the effect of woody vegetation on SSM retrievals and proposes a masking method at the native resolution of Sentinel-1's Interferometric Wide (IW) swath mode. At a continental 20 m grid, four dense vegetation masks are implemented over Europe in the resampling of the backscatter to a kilometre scale. The resulting backscatter is then used as input for the TUWien (TUW) change detection model and compared to both in-situ and modelled SSM. This paper highlights the potential of high-resolution vegetation datasets to mask for non-soil moisture-sensitive pixels at a sub-kilometre resolution. Results show that both correlation and seasonality of the retrieved SSM are improved by masking the dense vegetation at a 20 m resolution.

HIGHLIGHTS

- Dense vegetation reduces the ability to retrieve surface soil moisture at a kilometre scale from Sentinel-1 backscatter which is currently available on the Copernicus Global Land Service portal.
- Applying selective masking for vegetation during the resampling phase improves Sentinel-1 sensitivity to soil moisture.
- A novel vegetation-corrected Sentinel-1 surface soil moisture product is processed over Europe for the period 2016–2022 included.
- The Sentinel-1 forest mask improves the Sentinel-1 SSM product correlation and seasonality compared to both modelled and in-situ datasets.

ARTICLE HISTORY

Received 1 November 2023
Accepted 27 December 2023



KEYWORDS

Synthetic Aperture Radar; soil moisture; vegetation; Sentinel-1; change detection; high-resolution

Introduction

Surface soil moisture (SSM) is a key variable controlling water and energy flux at the interface of the atmosphere and lithosphere (Robock et al., 2000). Defined as the water contained in the unsaturated soil surface, SSM regulates environmental processes such as precipitation, runoff, temperature, and evapotranspiration (Seneviratne et al., 2010). Its accurate monitoring is valuable for a vast range of environmental applications, such as hydrological modelling (Alfieri et al. 2022; Laiolo et al. 2016), drought monitoring (Vreugdenhil et al. 2022; Yuan et al. 2015), crop management and irrigation (Dari et al. 2023; Ge et al. 2011) and flood forecasting (Ford and Quiring, 2019; Kim et al. 2019). Over the last decades, microwave remote sensing became a reliable technology to estimate soil water content at a global scale with high temporal resolution (Peng et al. 2020). Exploiting the difference between the dielectric

properties of soil and water, active microwave retrievals are able to provide global SSM data over time with a frequency independent from cloud cover and seasonal daylight variability (Karthikeyan et al. 2017). As part of Copernicus, the European earth observation program, ESA's Sentinel-1A and -1B satellites were launched into orbit in 2014 and 2016, respectively. Additionally, Sentinel-1C and -1D are in the development phase and planned to be launched in this decade ensuring the continuation of the mission. In December 2021, Sentinel-1B's mission was ended due to anomalies of the instruments on-board. Following the heritage of Envisat Advanced Synthetic Aperture Radar (ASAR), the Sentinel-1 (S1) constellation (S1) provides unprecedented multi-looked ground range resolution of 20 m by 22 m (Torres et al. 2012). It became apparent that monitoring SSM at near-real-time using the Sentinel-1 satellites has high potential (Hornacek et al. 2012). Building

CONTACT Samuel Massart  samuel.massart@geo.tuwien.ac.at  Department of Geodesy and Geoinformation, Vienna University of Technology, Technische Universität Wien, Wiedner Hauptstraße 8-10, Franz-Grill-Straße 9, 1030, Vienna 1040, Austria

© 2024 The Author(s). Published by Informa UK Limited, trading as Taylor & Francis Group.

This is an Open Access article distributed under the terms of the Creative Commons Attribution License (<http://creativecommons.org/licenses/by/4.0/>), which permits unrestricted use, distribution, and reproduction in any medium, provided the original work is properly cited. The terms on which this article has been published allow the posting of the Accepted Manuscript in a repository by the author(s) or with their consent.

upon the TUW change detection model from Wagner et al. (1999), Pathe et al. (2009), and Hornacek et al. (2012), Bauer-Marschallinger et al. (2019) developed an SSM product based on the linear relationship between Sentinel-1 backscatter and soil water content. In this algorithm, the Sentinel-1 backscatter is first resampled to a 500 m sampling (1 km resolution) and then used as input for the TUW change detection model. The product showed satisfactory results compared to in-situ measurements and is currently available on the Copernicus Global Land Service (CGLS) Website¹ over Europe from 2015 onward.

One challenge faced when using microwave remote sensing data is the decreased sensitivity to soil moisture over dense vegetation (Bauer-Marschallinger et al. 2019). For upcoming high-resolution Synthetic Aperture Radar (SAR) missions like NASA's NISAR, Lal et al. (2023) states that dense vegetation content will reduce the ability for the satellite to monitor soil moisture. High biomass content leads to backscatter saturation and the SAR is not able to penetrate the canopy layer. Additionally, most operational soil moisture products from microwave observations, such as the ESA's CCI soil moisture², and SMAP soil moisture³ or EUMETSAT's soil moisture product⁴, mask dense forests and high biomass content.

To retrieve SSM from Sentinel-1, different masking approaches have been tested to retrieve SSM from the backscatter signal while accounting for vegetation contribution at a kilometre scale. The implementation of radiative transfer theory allows to physically model vegetation temporal dynamics and thus improve SSM retrievals. These approaches are typically more computationally intensive but have shown positive improvements at the plot scale (Chatterjee et al. 2020; Foucras et al. 2020), or regional scale (Quast et al. 2023). Alternatively, machine-learning approaches use the backscatter information to retrieve SSM using varying model complexity from statistical regression (Nguyen et al. 2021), supervised ensemble learning (Hajdu et al. 2018) or unsupervised neural networks (Hegazi et al. 2021). Physical and machine learning-based models show validation improvements with regard to models that do not actively account for vegetation in the backscatter signal. However, either these models are not tested over pixels with dense forested content; either they show poor validation over forest pixels when compared to croplands, shrublands or grasslands pixels.

The CGLS soil moisture also performs poorly over areas with complex vegetation geometry compared to both modelled and in-situ soil moisture (Bauer-Marschallinger, 2022). Seasonal patterns introduce temporal biases due to vegetation changes in the soil

moisture time series. Where coarse resolution microwave data need to mask entire pixels, the high-resolution Sentinel-1 data and the current algorithm used for the operational CGLS SSM enable masking backscatter at the original resolution of Sentinel-1, i.e. before resampling to 500 m.

This paper investigates the impact of vegetation on S1 backscatter and subsequent SSM retrievals. The study highlights the benefits of masking 20 m resolution backscatter pixels with low sensitivity to surface soil moisture due to dense vegetation. Three different vegetation datasets derived from optical or microwave data are tested as high-resolution vegetation masks. These SSM datasets are validated using in-situ soil moisture from the International Soil Moisture Network (ISMN) and used to select the best performing mask. This mask is used to retrieve soil moisture over Europe at 500 m (to the same extent as the Copernicus Global Land Monitoring (CGLS) SSM product), and its performance is evaluated against ERA5-Land SSM (Muñoz-Sabater et al. 2021) relative to the benchmark of CGLS SSM.

This study shows that by discarding pixels flagged with a strong vegetation signal before resampling the backscatter to a kilometre scale, Sentinel-1 SSM shows better agreement with both, in-situ, and modelled SSM. We therefore propose a novel

Sentinel-1 SSM product including dense vegetation masking at 20 m resolution.

Materials

Sentinel-1 backscatter and preprocessing

The Sentinel-1 satellites are part of the Copernicus Sentinel constellation carrying C-band SAR. Compared to older missions (e.g. Envisat ASAR), Sentinel-1 is characterized by higher revisit times, higher spatial resolution, and continuity in the form of Sentinel-1C and Sentinel-1D planned to be launched in the next decade (Torres et al. 2012). The Sentinel-1 satellites are equipped with C-band SAR sensors working at a frequency of 5.405 Hz and measuring both cross- (VV) and co- polarization (VH) backscatter. In their IW swath mode, the sensors measure multi-looked backscatter at a ground range detected resolution of 20 m by 22 m resolution, at incidence angles from 29° to 46° over flat terrain, covering a swath of 250 km. When both Sentinel-1A and -1B were operational, revisit time varied between 1.5 and 4 days over Europe. The backscatter dataset used in this study originates from the backscatter dataset utilized in the production of CGLS SSM (Bauer-Marschallinger et al. 2018).

¹<https://land.copernicus.eu/global/products/ssm>

²<https://climate.esa.int/en/projects/soil-moisture/>

³<https://smap.jpl.nasa.gov/data/>

⁴<https://navigator.eumetsat.int/product/EO:EUM:DAT:METOP:SOMO12>

Within the CGLS SSM processing chain, the Sentinel-1 data from 2016 to 2021 (included) are radiometrically calibrated and terrain corrected using the Shuttle Radar Topography Mission (SRTM) Digital Elevation Model (DEM) at 90 m resolution. The preprocessed data consists of georeferenced σ^0 backscatter and a local incidence angle (θ) at 20 m sampling and is stored as datacube in the Equi7Grid framework (Bauer-Marschallinger et al. 2014). An additional filtering step is added to the VV polarised backscatter to discard pixels with extreme backscatter values below -20°dB and above -5°dB . The reasoning behind this is that high backscatter values likely originate from cities and other man-made objects that act as corner reflectors, low backscatter values are predominantly caused by water bodies and other non-soil surfaces.

Sentinel-1 CGLS SSM

The default Sentinel-1 CGLS SSM data, available on the CGLS website⁵, is used as a benchmark. The CGLS SSM product is based on the assumption that the temporal variability of the backscatter coefficient σ^0 (in decibels) is related to SSM changes in the surface soil layer. Vegetation, geometry, and roughness are assumed to behave as static, allowing for a simpler parametrization, which does not require external datasets or iterative adjustments. SSM is calculated by scaling backscatter between the driest and wettest soil conditions, i.e. the lowest and highest observed backscatter at certain incidence angles. For more details on the SSM retrievals, we refer to Bauer-Marschallinger et al. (2019).

Reference data

International soil moisture network

The International Soil Moisture Network (ISMN) is a global soil moisture database providing data from more than 2800 stations across 71 networks worldwide (as of 1 January 2023). The data is continuously updated, harmonised and freely available⁶ All ISMN SSM measurements are subjected to an automated quality control using a standardised flagging system removing out of range values, geophysical inconsistencies and outliers (Dorigo et al. 2011, 2021). In this paper, only the networks fulfilling the following requirement are used:

- Sensors located on the European continent. (-12° to 42°E and 35° to 72°N)
- Sensors located within the uppermost 10 centimetres of the soil.

- If multiple sensors are available at the exact same coordinates, only the sensors at the shallower depth are considered. If multiple sensors are available at equivalent depth, the sensor with the highest number of measurement is considered for the given coordinates.
- Sensors operational for at least 1 year of SSM data since the launch of Sentinel-1.
- At least 100 backscatter observations from Sentinel-1 are available during the operational time-span of the sensor.
- Sensors located within 500 m Sentinel-1 pixels displaying a percentage of forest masked between 10% and 99% (at 20 m sampling). Above 99%, the Sentinel-1 data are discarded. Below 10%, the impact of the forest masking is marginal on the backscatter dynamics as the majority of resampled pixel is not dominated by dense vegetation.

Table 1 summarizes the number of available stations fulfilling the above-mentioned requirements.

ERA5-land surface soil moisture

ERA5-Land is the first operational land reanalysis part of the ERA5 series from the European Centre for Medium-Range Weather Forecasts (ECMWF) produced within the Copernicus Climate Change Service (C3S), based on a 9 km grid spacing ($0.1^\circ \times 0.1^\circ$), and covering a period from 1950 to 2022 included (as of 1 April 2023) (Muñoz-Sabater et al. 2021). ERA5 Land uses Carbon Hydrology-Tiled ECMWF Scheme for Surface Exchanges over Land (CHTESSEL) to partition the water and energy fluxes over land, thus providing 50 land variables at an hourly temporal resolution. The land surface model is driven by meteorological forcing from ERA5 including precipitation, air temperature, humidity wind speed, and surface fluxes. The variable selected for the Sentinel-1 SSM validation is the volumetric soil water at a depth of 0–7 cm [m (Baghdadi et al., 2018)/m (Baghdadi et al., 2018)]. ERA5-Land soil moisture was validated using in-situ measurements from ISMN between 2010 and 2018 showing satisfactory results and slight improvements compared to its predecessor ERA5-Interim (Muñoz-Sabater et al. 2021).

Vegetation datasets

Sentinel-1 based forest map

The Sentinel-1 forest map is derived using both VV- and VH-polarised 20 m resolution backscatter from 2017 (Dostálová et al. 2021). Regions with similar vegetation and environmental characteristics were

⁵<https://land.copernicus.eu/global/products/ssm>

⁶<https://ismn.earth/en/>.

Table 1. Stations considered for the in-situ validation of the forest mask sentinel-1 SSM.

Network	Stations	Time-extent	Dominant Land Cover
HOBE	35	01.01.2015–10.08.2019	1. Tree cover, needleleaved, evergreen, closed to open (>15%) 2. Cropland, rainfed
IPE	2	01.01.2015 –25.03.2020	1. Tree cover, needleleaved, evergreen, closed to open (>15%) 2. Cropland, rainfed
RSMN	5	01.01.2015 –12.31.2022	1. Cropland, rainfed 2. Urban areas
SMOSMANIA	16	01.01.2015 –01.01.2021	1. Tree cover, needleleaved, evergreen, closed to open (>15%) 2. Cropland, rainfed 3. Grasslands
REMEDHUS	2	01.01.2015 –01.01.2022	1. Cropland rainfed 2. Cropland irrigated or post-flooding
HOAL	3	01.01.2015 –12.31.2021	1. Cropland rainfed
FMI	8	01.01.2015 –12.31.2022	1. Shrub or herbaceous cover, flooded,fresh/saline/brackish water 2. Mosaic tree and shrub (>50%), herbaceous cover (<50%) 3. Tree cover, needleleaved, evergreen, closed to open (>15%)
WSMN	2	01.01.2015 –29.02.2016	1. Grassland 2. Urban areas
TERENO	2	01.01.2015 –06.07.2021	1. Grassland 2. Cropland rainfed
FR-Aqui	3	01.01.2015 –01.01.2022	1. Tree cover, needleleaved, evergreen, closed to open (>15%)
BIEBRZA_S-1	1	03.04.2015 –01.12.2018	1. Shrub or herbaceous cover, flooded,fresh/saline/brackish water 2. Grassland

manually delineated. For each region, backscatter temporal signature was defined for both coniferous and deciduous forests using averaged backscatter every 12 days over 30 by 30 forested pixels. The seasonality of each pixel was then compared to regional prototype forest signature (broadleaved, coniferous) and then assigned to the most likely signature. High accuracy was found over Central and Eastern Europe between the Sentinel-1-based forest map and national forests map, as well as the Copernicus HRL dataset.

ESA's WorldCover map

ESA's WorldCover map is a global land cover map for 2020 at 10 m sampling based on the synergistic use of Sentinel-1 and Sentinel-2. One hundred and six features are extracted from Sentinel-1 and Sentinel-2 based on descriptive statistics (quantiles, range) as well as long-term averages. An additional 25 features are extracted from auxiliary datasets (Copernicus DEM, OpenStreetMap, Global Human Settlement Layer, Global Surface Water Explorer, Global Mangrove Watch). These features are ingested to train a classification algorithm resulting in a 10 m sampling land cover map with 11 classes and an overall accuracy surpassing 75% (The complete description of the algorithm is available in the product user manual on the ESA's WorldCover website⁷).

The forested class from the WorldCover map is defined as: “any geographic area dominated by trees with a cover of 10% or more. Other land cover classes (shrubs and/or herbs in the understorey, built-up, permanent water bodies, etc.) can be present below the canopy, even with a density higher than trees. Areas planted with trees for afforestation purposes and

plantations (e.g. oil palm, olive trees) are included in this class. This class also includes tree covered areas seasonally or permanently flooded with fresh water except for mangroves.”(Zanaga et al., 2022).

Copernicus land monitoring service – tree cover density

The Copernicus Tree Cover Density dataset is provided by the Copernicus Land Monitoring Service (CLMS) and is included in the Pan-European High-Resolution Layers (HRL). The dataset provides a 10 m sampling European map of the proportional crown coverage, also defined as the “vertical projection of tree crowns to a horizontal earth's surface”. The data is processed using 2018's Sentinel-2 time series. Fifty-nine statistical features are extracted and ingested in a random forest classifier with 200 decision-trees. First, a binary tree-cover map is produced, and then a tree-cover density is attributed to each pixel within the tree-cover mask. Validation showed that results are stronger over central Europe and lower for Western and Southern Europe (Sannier and Pennec, 2017).

CORINE land cover

The CORINE Land Cover (CLC) map is provided by the CLMS at a 100 m sampling based on Sentinel-2 and Landsat-8. The dataset consists in 44 standardized land cover classes over Europe. The CLC has a minimum feature width of 100 m and a minimum mapping unit of 25 ha. The mapping and land cover classification is carried out by national experts using varying techniques. It follows technical standards and nomenclature to provide a harmonized pan-European dataset. The CLC map released in 2018 is the fifth

⁷https://worldcover2020.esa.int/data/docs/WorldCover_PUM_V1.1.pdf

iteration of the dataset and provides a thematic accuracy of >85% (Büttner, 2014). Compared to the ESA WorldCover map described in 2.4.2: On the one hand, the CLC map provides additional information with regard to forest content. Each forested pixel is subdivided into broadleaved, coniferous or mixed forests. On the other hand, the dataset is provided at a coarser resolution compared to the ESA WorldCover map.

Methods

Vegetation mask standardisation

To integrate the high-resolution vegetation products described in Section 2.4 in the resampling processing chain, they are converted to binary arrays of forest and non-forest pixels. The Sentinel-1 forest mask (S1-mask) is created by combining the pixels defined as coniferous and broadleaved forest into a binary layer. For the ESA's WorldCover Map, the "Tree cover" land cover class is converted into a binary mask (WC-masked SSM). The Tree Cover Density Map provides continuous crown coverage values. Hence, two binary maps are derived based on different percentage thresholds, 30%, and 70%, respectively (TC30-masked SSM, TC70-masked SSM). All dense forest masks are resampled to Equi7Grid standard (Bauer-Marschallinger et al. 2014) to match the Sentinel-1 backscatter data.

Resampling and soil moisture retrievals

Operational SSM estimation at the continental-scale demands for robust and efficient retrieval algorithms. With respect to the complexity of the SAR signal at the native high resolution – with highly dynamic interactions between and within soil and vegetation – a downscaling to the kilometric scale increases the reliability of the SSM signal, as done e.g. within the CGLS product. The resampling of the Sentinel-1 scenes from the initial 20 m sampling to a 500 m pixel spacing decreases uncertainties caused by speckle, ground variability from soil roughness, or non-soil features. Furthermore, it significantly reduces the data volume and allows for a much more efficient processing in the near-real-time operations.

However, a suitable masking of the "raw" backscatter observations at the 20 m sampling give the possibility to filter for signal components relevant to SSM retrieval. The 20 m input backscatter is masked with the different dense vegetation masks described in 2.4. Any pixels flagged as dense vegetation are discarded from the resampling. If more than 99% of the pixels are discarded, the resulting resampled pixel is classified as "no data". The suitable pixels are arithmetically averaged in the linear domain for each Sentinel-1 scene and a 3 by

3 Gaussian filter is applied to the resampled 500 m products to reduce aliasing effects.

The soil moisture is retrieved in the same manner as for the CGLS soil moisture product. To obtain SSM observations, each backscatter scene is normalized to a common reference angle of 40°. Normalizing each data point to a common incidence angle is essential to compare the temporal evolution of the backscatter coefficient σ^0 , as each resampled backscatter value is strongly related to the incidence angle at which it is observed. To do so, the relationship between backscatter coefficients and local incidence angles is assumed to be linear (Bauer-Marschallinger et al. 2019). The revisit time (thus the number of observations) being inhomogeneous, some areas only have measurements with two distinct local incidence angles making it impossible to fit a linear regression. Bauer-Marschallinger et al. (2019) introduced an alternative approach to estimate the linear slope (β_r) using the mean and sensitivity of σ^0 .

The observed normalized backscatter is then scaled between the wet and dry references, which define the theoretical extreme soil moisture states of a given pixel. The potential of outliers, artificially extending the wet and dry parameters range, is mitigated by selecting the 10th and 90th percentile as wet and dry references. From these percentiles, the 0th and 100th percentile of SSM is then linearly interpolated as described in the following equations.

$$\sigma_{dry}^o = \sigma_{10}^o - \frac{10}{80} * (\sigma_{90}^o - \sigma_{10}^o) \quad (1)$$

$$\sigma_{wet}^o = \sigma_{90}^o + \frac{10}{80} * (\sigma_{90}^o - \sigma_{10}^o) \quad (2)$$

Finally, SSM is extracted for each normalized backscatter scene.

$$SSM(t) = \frac{\sigma^o(t) - \sigma_{dry}^o}{\sigma_{wet}^o - \sigma_{dry}^o} \quad (3)$$

Evaluation of the masked products

The impact of masking dense vegetation on the Sentinel-1 SSM is evaluated in a two-step approach. First, a per-station evaluation is done based on in-situ soil moisture. Second, the best performing masking approach is evaluated over Europe against the ERA5-Land SSM product. For the evaluation, the CGLS SSM is considered as benchmark, and any improvements or deterioration are quantified with respect to this dataset.

In-situ evaluation

The selected in-situ stations from 2.3.1 are paired with their relative resampled Sentinel-1 pixel. A station is included for the validation process if, during the

resampling phase, its matching Sentinel-1 pixel had between 10% and 99% of its data masked as dense vegetation by all three masks. This criterion ensures that the resampling correction has an impact on the backscatter values. Pixels outside of the 10–99% masking range either are marginally impacted by the vegetation mask or the entire pixel is fully discarded. The SSM products are scaled to in-situ soil moisture using a mean standard deviation scaling. For each suitable station, Pearson correlation coefficients are computed. The correlation changes for each in-situ station are compared to the percentage of pixels discarded using the Sentinel-1 forest mask to assess the effect of the reduction of available pixels during the resampling phase.

Large-scale evaluation

To conduct a large-scale evaluation of the SSM product, we selected the most skilful vegetation mask based on in-situ analysis. The masking approach based on the Sentinel 1 forest mask is evaluated using the ERA5-Land SSM product across Europe to assess potential impacts on the accuracy and reliability of the SSM product. Each Sentinel-1 pixel is matched to its nearest ERA5-Land pixel. The resolution of ERA5 Land is 0.1° by 0.1° meaning that multiple Sentinel-1 pixels are matched to a single ERA5-Land time series. Each Sentinel-1 scene is matched with the temporally closest ERA5-Land observation with a maximum masking time difference of 6 hours for two observations to be matched. If the ERA5-Land soil temperature is below 3°C , the coupled observations are discarded. For each resulting time series, Pearson correlations are computed. The Sentinel-1 SSM datasets are scaled (with mean-standard deviation scaling).

The large-scale evaluation is done both on the full time series and per season. For each season, the Pearson correlation and bias are computed. To detect if the bias is reduced through dense vegetation masking, the absolute values of the biases per season are calculated for the benchmark and masked SSM products. If the absolute bias from the new product is closer to 0 than the bias of the benchmark product, then the vegetation masking positively corrects for bias. To estimate the impact of climate (and potential seasonal dynamics) on the skill of the SSM retrieval, the correlations are spatially grouped and averaged for climatic region based on the Köppen – Geiger classification.

Results

In-situ evaluation

Figure 1 shows the correlation coefficients with in-situ soil moisture for each station, comparing the SSM products processed with the vegetation masks to the

CGLS SSM benchmark. For the majority of the in-situ stations the correlation increases regardless of the masking approach. The correlation improvement is consistently positive when the pixels show an initial correlation of $\rho > 0.4$ compared to the benchmark CGLS SSM. However, if ρ is initially low ($\rho < 0.4$), the vegetation masking approach becomes inconsistent. The average correlation for all stations with the CGLS SSM is 0.372. Note that the low correlation stems from the selection of the stations as we only consider stations within pixels with a minimum forest content. The addition of croplands and grasslands station would likely increase the average correlation. The S1-masked and WC-masked SSM products perform better, with the same average correlation coefficient of 0.435. The TC30- and TC70-masked SSM products (see Table 2) show also an improvement compared to the CGLS SSM benchmark, albeit slightly lower than for the S1 and WC-mask, with 0.427 and 0.416 correlation coefficients, respectively.

The improvement in correlation increases along with the percentage of dense vegetation pixels masked within the 500 m pixel, as the largest points are located closest to the 1:1 line. Larger correlation improvements are observed over pixels with high percentages of masked vegetation. The networks HOBE and SMOSMANIA are good examples where applying a vegetation mask during the resampling phase improves Sentinel-1 skills to monitor SSM. These two networks are located in humid continental climates (Dfb, Cfb) with clear seasonal dynamics. In these regions, the forested pixels show no clear seasonality in soil moisture dynamics, due to the attenuation of the signal by the vegetation. Figures 2 and 3 show two case studies comparing in-situ soil moisture against the CGLS SSM benchmark and the S1-masked SSM for a station in France (SMOSMANIA, LaGrandCombe) and Finland (FMI, SOD012). The soil moisture sensitivity over LaGrandCombe is largely improved thanks to the vegetation mask, with improvements in ρ from 0.135 to 0.528. In the S1-masked SSM, the sensitivity to seasonal soil moisture dynamics is improved, with high soil moisture in winter and low soil moisture in summer. This is shown in Figure 2(a) as compared to Figure 2(b), where the seasonal dynamics that are present in the in-situ soil moisture are not represented in the CGLS SSM data. At FMI, there is no clear improvement in ρ . In addition, no improvements in seasonal dynamics can be observed and the entire winter season is masked. The time series indicates that the validation period is constrained from May to November due to the low-temperature masks from both ERA5-Land and ISMN. During these months, the S1 sensitivity to in-situ soil moisture is initially low ($\rho = 0.157$) and is further decreased after masking for dense vegetation ($\rho = 0.036$). For each FMI sensors, the initial in-situ correlation is below 0.2 and the percentage of masked pixels is high. A decrease in

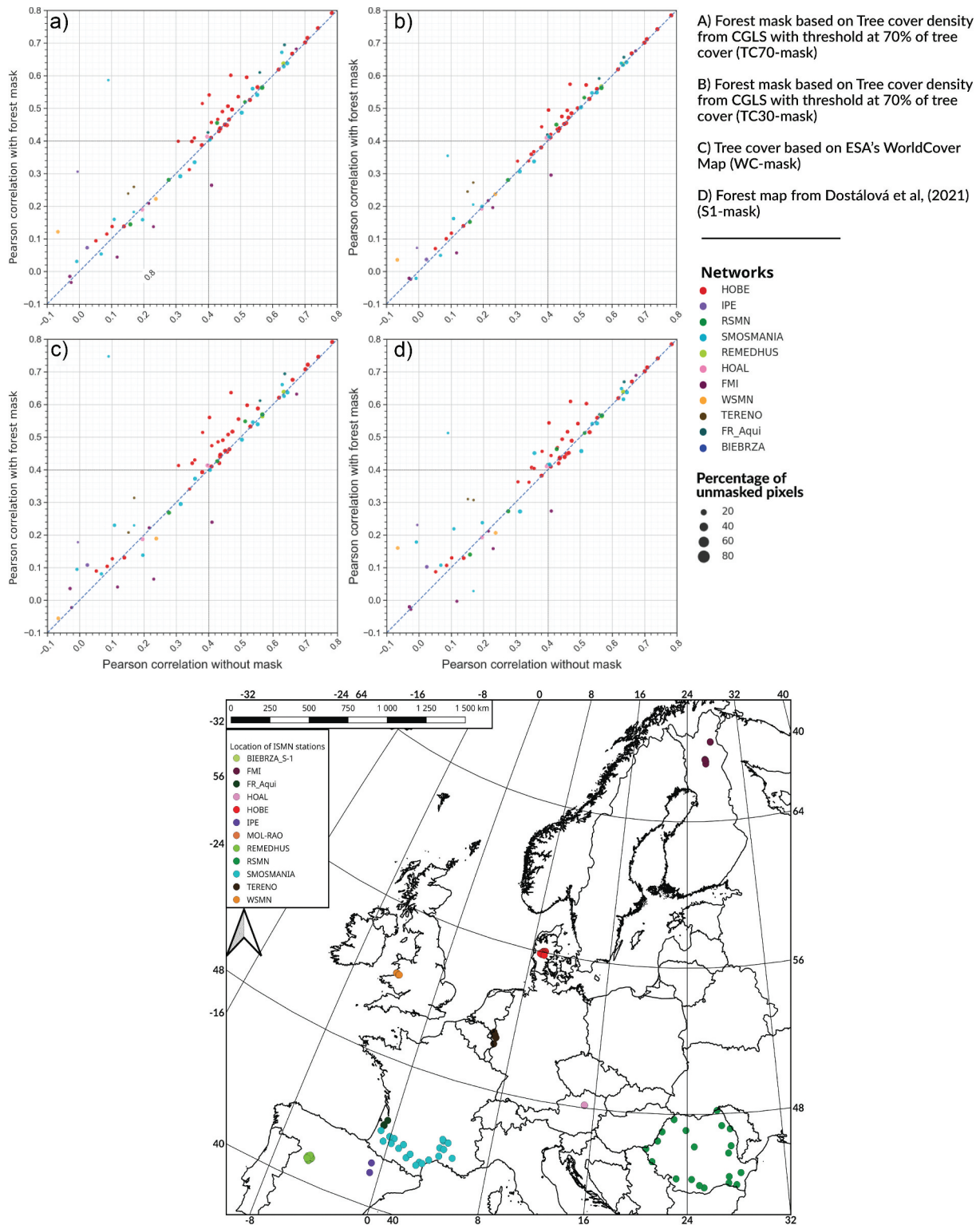


Figure 1. Comparison of the correlation between ISMN in-situ stations with default SSM and (x-axis) and vegetation masked SSM (y-axis) using the 4 different masking approaches. The point coloration denotes to which ISMN network the station belongs. The size of the point represents the percentage of 20m pixels selected during the resampling phase to produce the kilometre scale product. The plotted points located above the diagonal line indicates that the vegetation mask has a positive impact on the soil moisture retrieval.

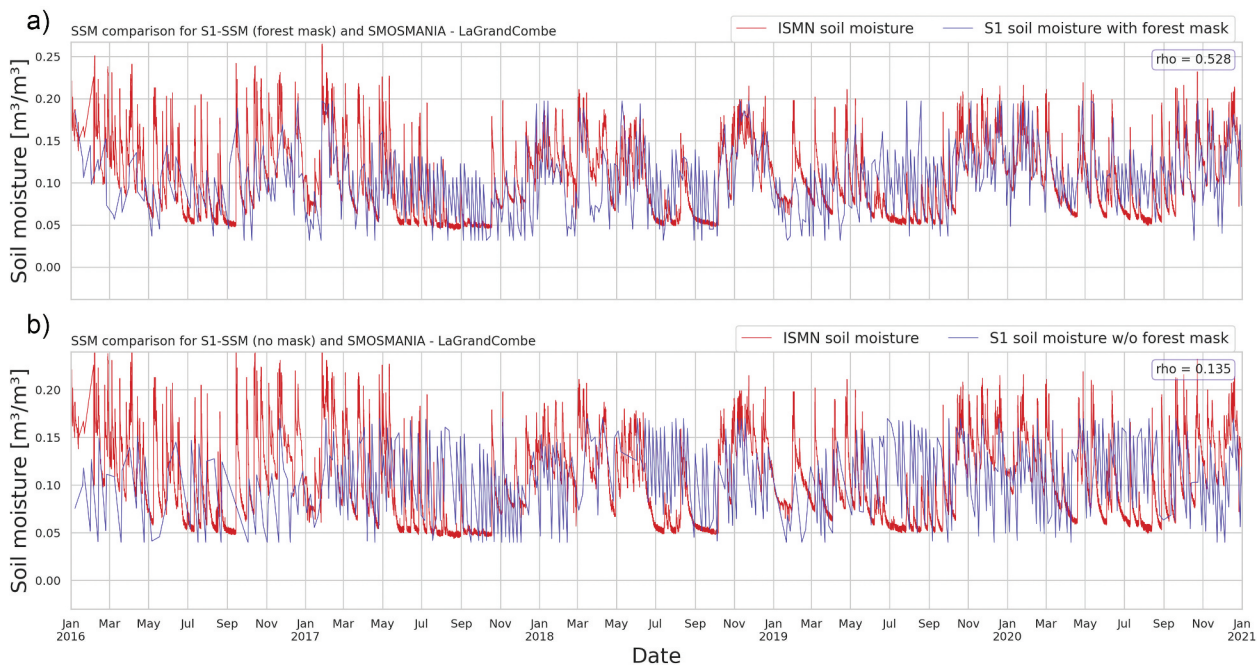
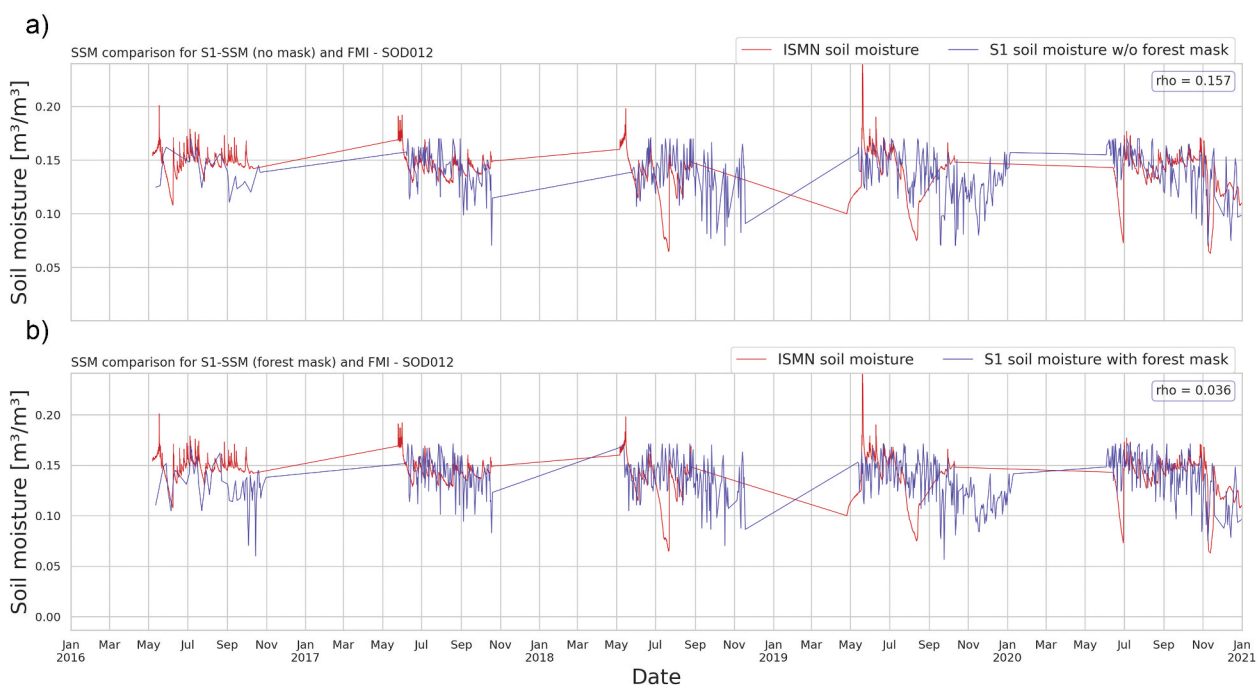
correlation coefficients is observed regardless of the masking approach ($\hat{p}_{\text{default}} = 0.190$ compared to $\hat{p}_{\text{TC70}} = 0.156$, $\hat{p}_{\text{TC30}} = 0.128$, and $\hat{p}_{\text{S1}} = 0.134$). In these landscapes, dense vegetation does not seem to be the leading cause of low SSM sensitivity and is likely not the only source of noise in the observed signal.

Large-scale evaluation

To estimate the sensitivity of S1-masked SSM to seasonal dynamics over Europe the CGLS and S1-masked SSM are compared to ERA5-Land SSM. Figure 4 shows the correlation map between ERA5-Land to

Table 2. Performances of the different masking approaches over the ISMN stations.

	Avg. Pearson (in-situ)	Avg. Pearson (ERA5-Land)	Avg. Spearman (in-situ)	Avg. Spearman (ERA5-Land)
Benchmark	0.372	0.408	0.383	0.470
WC mask	0.435	0.482	0.445	0.534
TC30 mask	0.427	0.470	0.436	0.522
TC70 mask	0.416	0.453	0.427	0.509
S1 mask	0.436	0.475	0.442	0.524

**Figure 2.** Comparison of the ISMN in-situ station “LaGrandCombe” from the network SMOS MANIA with: (a) the benchmark CGLS sentinel-1 SSM and (b) the vegetation corrected sentinel-1 SSM.**Figure 3.** Comparison of the ISMN in-situ station “SOD012” from the network FMI with: (a) the benchmark CGLS sentinel-1 SSM and (b) the vegetation corrected sentinel-1 SSM.

the benchmark CGLS SSM (A) and the S1-masked SSM (B). **Figure 4(c)** shows, for each km scale Sentinel-1 pixel, the percentage of 20 m pixels flagged and discarded as forested area prior to its resampling. Finally, **Figure 4(d)** shows the difference between **Figure 4(a,b)**. The areas coloured in blue indicate a positive effect of the dense vegetation masking on the S1-masked SSM correlation to ERA5-Land.

Figure 4(a) shows that the CGLS SSM has highest correlations over Central and Central-West Europe. Lower correlations are found in parts of South-eastern Spain and in Scandinavia. For the S1-masked SSM, similar spatial patterns are found in the correlation map. **Figure 4(d)** shows that the strongest increases in correlation coefficients using the S1-mask are found over Central and Northern Europe, parts of Spain, and Southern France. When compared to the CLC, these areas correspond mostly to coniferous forest and to a lesser extent to mixed and broadleaved forests (**Figure 5**). The S1-masked SSM has a significantly increased correlation coefficient compared to CGLS SSM, with largest improvements over coniferous forests. Dense vegetation masking lowers the impact of

the different forest types on the SSM retrievals, as the masked product displays average ρ above 0.4 ($\hat{\rho}_{\text{coniferous,masked}} = 0.410$, $\hat{\rho}_{\text{broadleaved,masked}} = 0.457$, and $\hat{\rho}_{\text{mixed,masked}} = 0.449$), as shown in **Figure 6**.

Figure 7 uses the data shown in **Figure 4(a,b)** mapped to the Köppen-Geiger climate classification. The largest increases are observed over the following climate types: Dfb (Warm-summer humid continental climate), starting from Eastern Germany and encompassing most of Eastern Europe, Bsk (Cold semi-arid climate) in Central Spain, and finally Csb (and to a lesser extent Csa) (Warm/Hot summer Mediterranean climate) in Portugal and Northern Spain. Overall, the correlation is consistently improved across the eco-regions with the exception of a very slight degradation over the humid subtropical climate (Cfa) in Northern Italy and Apulia.

Figure 8 shows the seasonal bias values between ERA5-Land, S1-masked SSM, and CGLS SSM (with standard deviation scaling to ERA5-Land). The bias between the two SSM products with regard to ERA5-Land SSM shows an underestimation of soil moisture in winter and spring, and an overestimation of soil

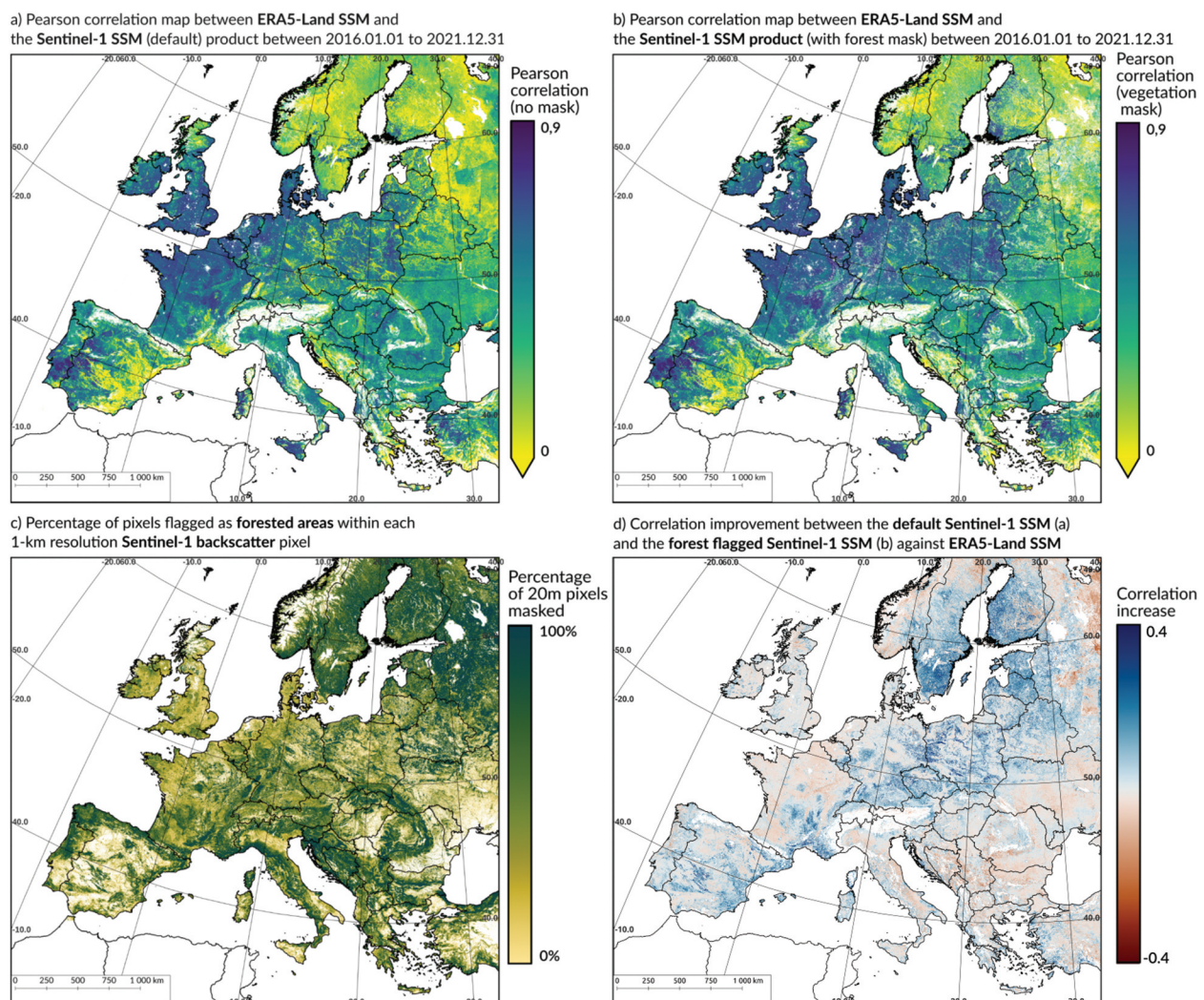


Figure 4. European results of sentinel-1 SSM with the addition of the S1-mask for vegetation.

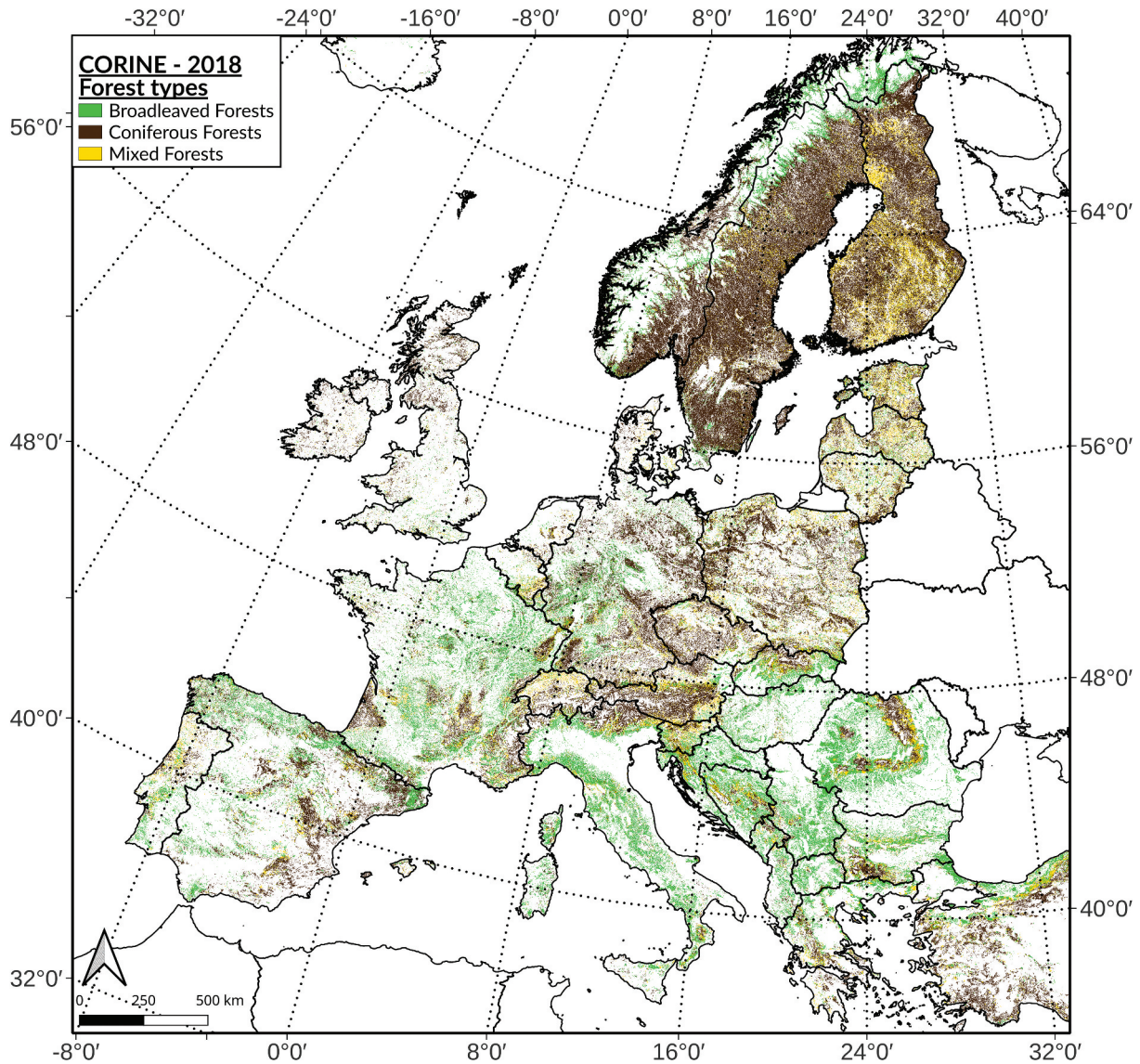


Figure 5. Comparison between broadleaved, coniferous and mixed forest based on the CORINE land cover map (2018).

moisture in summer. The third row is the difference between the absolute biases without and with masking for dense vegetation. If the difference in bias is negative, it means an improvement in bias for the masked SSM dataset, i.e. a bias closer to 0. Results show that, during winter and summer, masking for vegetation reduces the bias, i.e. the respective under- and over-estimations of SSM are decreased. This indicates that seasonality is improved.

Discussion

All soil moisture retrieval algorithms need to account for the vegetation contribution in their algorithm. Over vegetated soils, the microwave signal is the result of soil scattering, attenuation and scattering from the vegetation (Ulaby et al., 1986). Depending on the density of the vegetation, it is possible to model its effect on the soil moisture retrievals. Many approaches

have been tested to account and correct for vegetation scattering and attenuation on the Sentinel-1 backscatter signal at a kilometre scale. Combining data from optical (Ma et al. 2020; Madelon et al. 2023) or microwave (Bauer-Marschallinger et al. 2018; Zhu et al. 2022) sensors, utilizing advanced radiative transfer modelling (Mengen et al. 2023; Nguyen et al. 2021), or machine learning approaches (Chatterjee et al. 2020; Foucras et al. 2020), generally lead to improvements over croplands, grasslands and shrublands. These studies calibrate their models specifically for the aforementioned land covers, but show consistently poor soil moisture retrievals over complex vegetation structure. For dense and complex vegetation, microwave signals primarily detect dense vegetation geometry and seasonal effects. Operational coarse-scale soil moisture retrievals resolve this issue by masking soil moisture over pixels with dense vegetation (Dorigo et al. 2021).

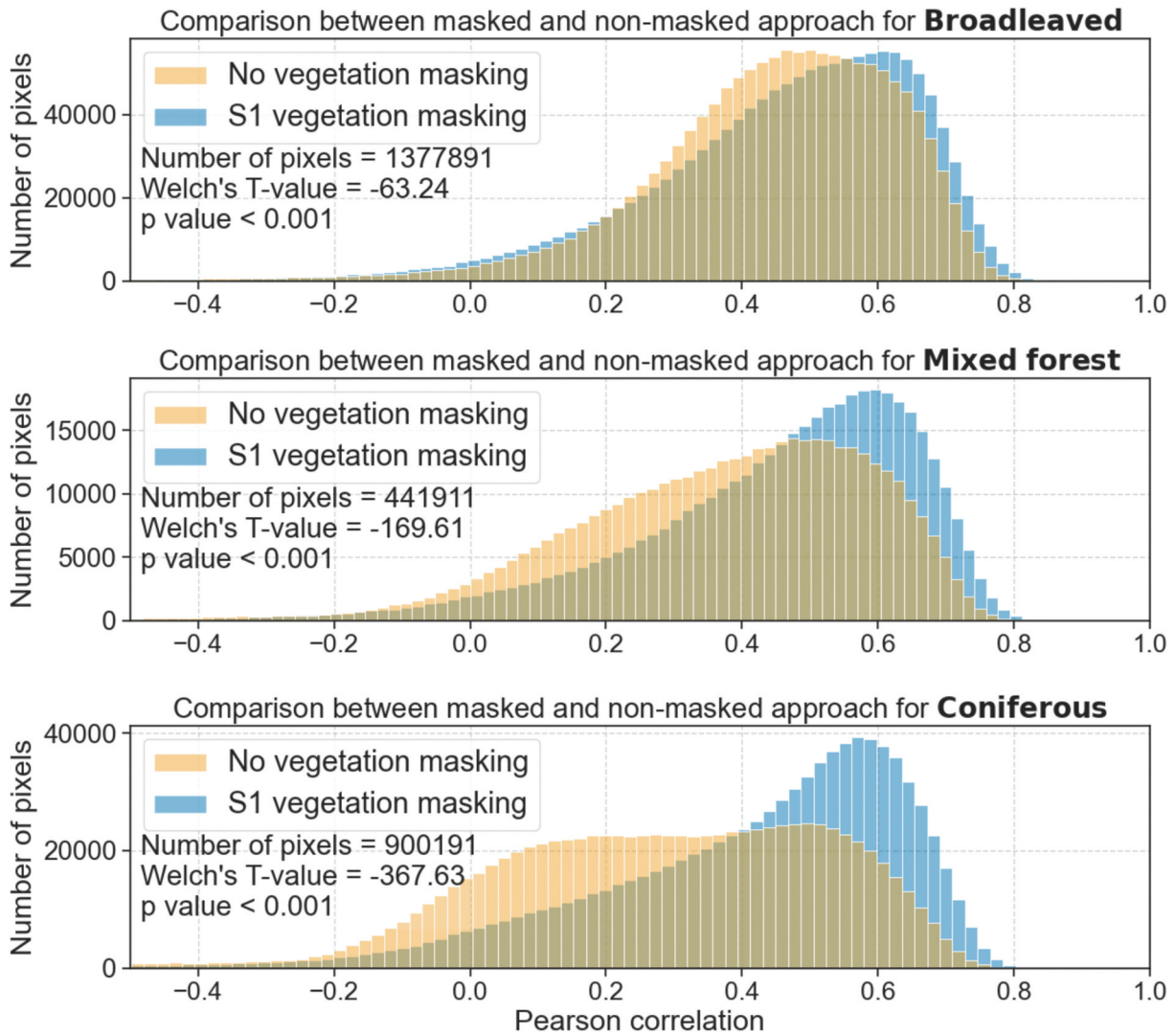


Figure 6. Comparison of the change in correlation for the pixels classified as forests in the CORINE land cover map (2018).

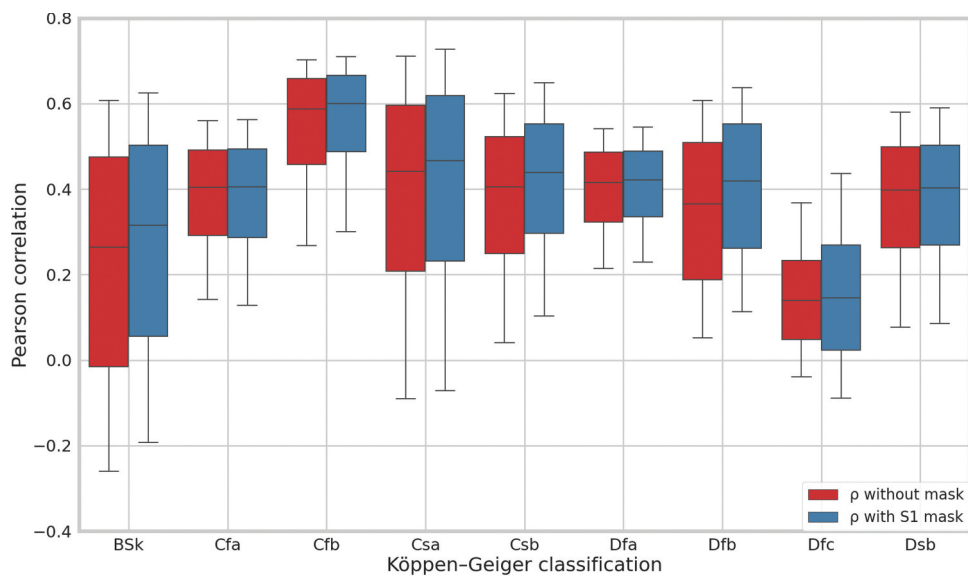


Figure 7. Averaged correlation between ERA5-land and S1-SSM (2016–2021 included) for the different köppen-Geiger climate regions of Europe. Each box represents the second and third quartile, the horizontal line is the median value and the whiskers show the 10th and 90th percentile. If the blue boxes are higher than their red counterpart, it indicates an increase in average correlation for the described climate class.

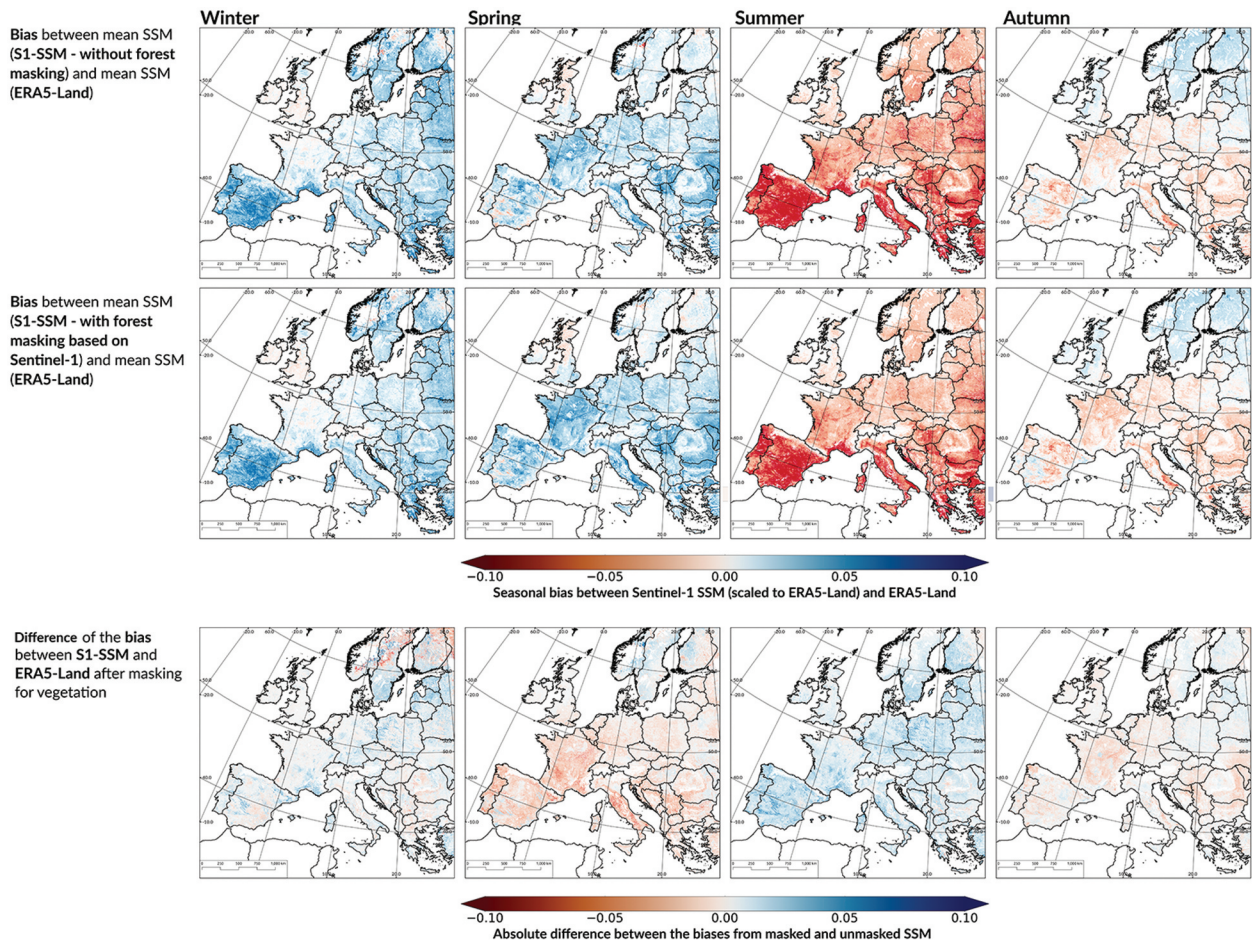


Figure 8. Summary of the seasonal bias analysis. The first row are the seasonal bias maps between the uncorrected SSM and ERA5-land. The second row shows the seasonal bias maps between the vegetation S1-masked SSM and ERA5-land. The third row is the absolute difference between the biases for benchmark and S1-masked SSM products (bias improvements).

The approach presented in this paper demonstrates the effect of dense vegetation on the soil moisture retrieval at high resolution and the potential to improve soil moisture retrieval by masking dense vegetation pixels at the backscatter level. The improvements in the SSM retrieval can be related to several effects: the choice of the vegetation mask and masking density, and the environmental variables such as climate and forest type. These will be discussed in the following sections.

Choice of vegetation mask and masking density

The validation against ISMN stations suggests that all vegetation-masking approaches have a positive impact on the correlation between Sentinel-1 SSM and in-situ observations. The four masks aim at categorizing the same forest land cover type, and, as shown in Figure 1, provide similar correlation improvements. The S1-mask (based on Sentinel-1) and WC-mask (based on Sentinel-1+Sentinel-2) perform slightly better compared to the TC30- and TC70-masks (based on Sentinel-2). The masks with better performances include Sentinel-1's VV

and VH temporal dynamics to infer the vegetation content of a pixel. An advantage of using the Sentinel-1 based vegetation mask is that the data source of the vegetation mask and the soil moisture retrieval is the same. Figure 1 shows that the improvement in correlation is closely related to the percentage of pixels that were masked during the resampling process. Where less than 10% of the pixels are masked, the resampled signal remains largely unchanged and the resulting change in correlation is minimal. However, where more than 50% of the pixels are masked, improvements are consistent, with the exception of FMI. The correlation map between ERA5-Land and the S1-masked SSM (Figure 4(b)), as well as the correlation improvement map in Figure 4(d) shows that, while the general spatial patterns of correlation remain similar, the impact of dense vegetation is reduced in the corrected SSM product. Even over pixels where 90% of pixels are discarded during the resampling phase, the remaining valid pixels resampled to the 500 m scale provide sufficient information to produce robust SSM signals that show a satisfactory correlation with ERA5-Land.

Impact of environmental conditions

Improvements of SSM for the different climate classes observed over the in-situ stations and ERA5-Land show similar patterns. Compared to ERA5-Land, Sentinel-1 performs poorly over subarctic climate, as it is the only climate type with a ρ below 0.2, even after vegetation masking. These results are consistent with the in-situ validation and with studies of Sentinel-1 SSM products over Northern in-situ networks (Nativel et al. 2022; Zhu et al. 2022). Low SSM sensitivity over these regions are linked to the subarctic climate (Dfc) as ephemeral lakes, and the annually low surface temperature are hindering SSM retrievals from microwave observations. Radar-based SSM retrievals are challenging over these areas as (nearly) frozen soils have a very low dielectric constant and are linked to a low backscatter. This reduces the ability of Sentinel-1 to estimate SSM over such climates (Baghdadi et al. 2018; Fayad et al. 2020), and masking of these conditions is needed. Long periods of freezing temperatures from autumn to spring lead to large data gaps, as shown in (Figure 3(a,b)). Because of the large data gaps, the forest masking approach does not provide consistent improvement and overall sensitivity to SSM remains low.

The other climate type with challenging SSM retrievals are semi-arid climates, which cover areas in southern Europe, particularly Spain and Italy. These areas correspond to areas where sub-surface scattering occurs as described by (Wagner et al. 2022). Here, the dry conditions lead to scattering from deeper soil layers, which increases backscatter (Morrison and Wagner, 2020), which is interpreted as high soil moisture in the change detection method. Nonetheless, the model validation shows improvements over temperate climates, with clear seasonal patterns. For instance, masking for vegetation over Oceanic, Mediterranean climates, and continental humid climate (Cfb, Csb and Dfb) shows good improvement when compared to both ERA5-Land (Figure 7) and the available ISMN networks (SMOSMANIA, HOBE, FR-Aqui and HOAL)

Effect of vegetation type

The benchmark CGLS product, especially the areas classified as coniferous or mixed forests according to the CORINE classification from 2018 (Figure 5), (EEA, 2018) show low correlations with ERA5-Land. Particularly mixed and coniferous forest benefit from masking the dense vegetation as their mean correlations are significantly increased. Multiple reasons can lead to the stronger improvement in coniferous forest compared to broadleaved forests. First, most coniferous forests in Europe are evergreen. Hence, attenuation of the microwave signal occurs throughout

the year. Broadleaved forests are mostly deciduous in Europe and the sensitivity to soil moisture may be higher when no leaves are on the trees. Secondly, forest biomass, defined as any biological matter produced by woody vegetation likely leads to higher signal attenuation. The integrated assessment of forest biomass in Europe provides information about the biomass content of European forests (Avitabile et al. 2020). Coniferous forests typically have a higher biomass content and the spatial patterns of Pearson correlation from Figure 4 closely follow the spatial patterns of forest biomass density. Additionally, according to the same report, the only two species whose estimated contributions are above 15% to the total European forest biomass are *Picea* sp, and *Pinus Sylvestris* (amongst the most common species in European coniferous forests). These results are consistent with the assumption that forests with higher biomass and denser vegetation have a stronger impact on the Sentinel-1 co-polarised backscatter signal.

This study shows that low correlations over forests can be resolved using the S1-based forest masking, as it can partially mitigate the seasonal bias between ERA5-Land and Sentinel-1 soil moisture. Nevertheless, vegetation masking does not completely resolve the vegetation issue. There is still a persisting bias during summer, which is likely due to a combination of the non-forested vegetation component, and orbit effects, which are not fully taken into account by the incidence angle normalisation process. Nonetheless, the dense forest masking decreases the Sentinel-1 wet bias during summer and to a lesser extent the dry bias during winter. This can be attributed to the low seasonal dynamics observed over forest with a dense vegetation, and high biomass, which contributes to the Sentinel-1 SSM seasonal bias (Dostálová et al. 2018; Rüetschi et al. 2017).

Conclusions

Vegetation water content, biomass density and surface soil moisture affect the temporal behaviour of the Sentinel-1 backscatter signal. In this study, we tested the potential of masking vegetation in the high-resolution backscatter images to reduce the impact of forests on the TUW change detection soil moisture retrievals, which is used in the CGLS operational soil moisture product. Results shows that masking dense vegetation prior to resampling the Sentinel-1 backscatter improves the quality of SSM retrievals at the kilometer scale. Four different tree cover maps were used for masking and the resulting soil moisture products were compared to in-situ soil moisture from the International Soil Moisture Network between 2016 and 2021. All four masks respectively based on Sentinel-1, Sentinel-2 or both show similar results, although slightly higher correlations are found using the Sentinel-1-based forest

mask. Satisfactory improvements are observed over the majority of stations, especially over networks in temperate and cold climates with a strong seasonality in vegetation and soil moisture. Vegetation masking does not lead to improvement over subarctic climates and semi-arid to arid climates, due to limitations in microwave remote sensing over frozen soils, snow covered soils, open water, and in dry areas prone to sub-surface scattering. The surface soil moisture product based on the backscatter filtered using the Sentinel-1 forest mask is then compared to ERA5-Land SSM over Europe. Overall, correlations are improved over pixels dominated by broadleaved, coniferous and mixed forests. The most pronounced correlation improvements are observed over coniferous forests, which have the highest aboveground biomass density among the different forest types in Europe. Masking for dense vegetation does not fully solve the seasonal biases between Sentinel-1 SSM and ERA5-Land, which can be attributed to the effects of non-forested vegetation and orbit patterns in the backscatter signal. While not fully solved, the wet and dry biases, during summer and winter respectively, are reduced by the implementation of dense vegetation masking.

This paper is another step to disentangling the effects of vegetation and SSM on the Sentinel-1 backscatter. Results suggest that the high resolution from Sentinel-1 can be used as an asset to selectively mask pixels with dominant vegetation effects on Sentinel-1 backscatter signal. This does not only apply for the CGLS soil moisture retrieval, as demonstrated in this study, but can also be applied to other retrieval algorithms. There is potential to apply a similar selective mask to reduce signal degradation from other sources. Subsurface scattering in semi-arid to arid-climate, as well as certain types of growing crops can also heavily influence the backscatter signal and reduce Sentinel-1 backscatter SSM sensitivity.

Disclosure statement

No potential conflict of interest was reported by the author(s).

Funding

This work is internally funded by the Department of Geodesy and Geoinformation of TU Wien and co-funded by the Copernicus Global Land Service under the Framework Service Contract N° 941115 - ISP- 2021 (JRC) and by the ESA “4DMed-Hydrology” project (contract n. 4000136272/21/I-EF). The authors acknowledge TU Wien Library for financial support through its Open Access Funding Program.

ORCID

Samuel Massart  <http://orcid.org/0009-0009-1312-5797>

Authors contributions

S.M. and M.V. conceptualized the research and designed the algorithm improvements. S.M. processed the improved product, performed the validation and wrote the first draft of the manuscript. CN and RN contributed to the Sentinel-1 preprocessing optimisation and helped developing the datasets. B.B.-M and W.W. helped for the methodology and model implementation. All authors contributed to the revision of the text and figures and approved the submission of the final manuscript.

Data availability statement

The data that support the findings of this study are available from the corresponding author, SM, upon reasonable request.

References

- Alfieri, L., Avanzi, F., Delogu, F., Gabellani, S., Bruno, G., Campo, L., Libertino, A., Massari, C., Tarpanelli, A., Rains, D., Miralles, D G., Quast, R., Vreugdenhil, M., Wu, H., Brocca, L., others. (2022). High-resolution satellite products improve hydrological modeling in northern Italy. *Hydrology and Earth System Sciences*, 26(14), 3921–3939. <https://doi.org/10.5194/hess-26-3921-2022>
- Avitabile, V., Camia, A., & Pilli, R. (2020). The biomass of European forests. An integrated assessment of forest biomass maps, field plots and national statistics. <https://doi.org/10.2760/311876>
- Baghdadi, N., Bazzi, H., El Hajj, M., & Zribi, M. (2018). Detection of frozen soil using sentinel-1 SAR data. *Remote Sensing*, 10(8), 1182. <https://doi.org/10.3390/rs10081182>
- Bauer-Marschallinger, B. (2022). Quality assessment report - update 2021 - surface soil moisture, collection 1km. *Copernicus Global Land Operations – “Vegetation and Energy”, Version 1.*
- Bauer-Marschallinger, B., Freeman, V., Cao, S., Paulik, C., Schaufler, S., Stachl, T., Modanesi, S., Massari, C., Ciabatta, L., Brocca, L., & Wagner, W. (2019). Toward global soil moisture monitoring with sentinel-1: Harnessing assets and overcoming obstacles. *IEEE Transactions on Geoscience and Remote Sensing*, 57(1), 520–539. <https://doi.org/10.1109/TGRS.2018.2858004>
- Bauer-Marschallinger, B., Paulik, C., Hochstöger, S., Mistelbauer, T., Modanesi, S., Ciabatta, L., Massari, C., Brocca, L., & Wagner, W. (2018). Soil moisture from fusion of scatterometer and SAR: Closing the scale gap with temporal filtering. *Remote Sensing*, 10(7), 1030. <https://doi.org/10.3390/rs10071030>
- Bauer-Marschallinger, B., Paulik, C., & Schaufler, S. (2018). *Copernicus global land operations “vegetation and energy”: Algorithm theoretical basis document: Surface soil moisture - collection 1km - version 1.0.*
- Bauer-Marschallinger, B., Sabel, D., & Wagner, W. (2014). Optimisation of global grids for high-resolution remote sensing data. *Computers and Geosciences*, 72, 84–93. <https://doi.org/10.1016/j.cageo.2014.07.005>

- Büttner, G. (2014). CORINE land cover and land cover change products. In *Land use and land cover mapping in Europe: Practices & trends* (pp. 55–74). Springer.
- Chatterjee, S., Huang, J., & Hartemink, A. E. (2020). Establishing an empirical model for surface soil moisture retrieval at the US climate reference network using sentinel-1 backscatter and ancillary data. *Remote Sensing*, 12(8), 1242. <https://doi.org/10.3390/rs12081242>
- Dari, J., Brocca, L., Modanesi, S., Massari, C., Tarpanelli, A., Barbetta, S., Quast, R., Vreugdenhil, M., Freeman, V., Barella-Ortiz, A., Quintana-Seguí, P., Bretreger, D., Volden, E., others. (2023). Regional data sets of high-resolution (1 and 6 km) irrigation estimates from space. *Earth System Science Data*, 15(4), 1555–1575. <https://doi.org/10.5194/essd-15-1555-2023>
- De Keersmaecker, D., Van De Kerchove, R., Zanaga, W., Souverijns, N., Brockmann, C., Quast, R., Wevers, J., Grosu, A., Paccini, A., Vergnaud, S., Cartus, O., Santoro, M., Fritz, S., Georgieva, I., Lesiv, M., Carter, S., Herold, M., Li, L., Tsendbazar, N.-E.; Arino, O. (2021). ESA WorldCover 10 m 2020 v100. *Nature Communications*, 12(1), Zenodo. <https://doi.org/10.5281/zenodo.5571936>
- Dorigo, W., Himmelbauer, I., Aberer, D., Schremmer, L., Petrakovic, I., Zappa, L., Preimesberger, W., Xaver, A., Annor, F., Ardö, J., Baldocchi, D., Bitelli, M., Blöschl, G., Bogena, H., Brocca, L., Calvet, J. C., Camarero, J. J., Capello, G., Choi, M., ... Sabia, R. (2021). The international soil moisture network: Serving earth system science for over a decade. *Hydrology and Earth System Sciences*, 25(11), 5749–5804. <https://doi.org/10.5194/hess-25-5749-2021>
- Dorigo, W. A., Wagner, W., Hohensinn, R., Hahn, S., Paulik, C., Xaver, A., Gruber, A., Drusch, M., Mecklenburg, S., Van Oevelen, P., Robock, A., & Jackson, T. (2011). The international soil moisture network: A data hosting facility for global in situ soil moisture measurements. *Hydrology and Earth System Sciences*, 15(5), 1675–1698. <https://doi.org/10.5194/hess-15-1675-2011>
- Dostálová, A., Lang, M., Ivanovs, J., Waser, L. T., & Wagner, W. (2021). European wide forest classification based on sentinel-1 data. *Remote Sensing*, 13(3), 1–27. <https://doi.org/10.3390/rs13030337>
- Dostálová, A., Wagner, W., Milenković, M., & Hollaus, M. (2018). Annual seasonality in sentinel-1 signal for forest mapping and forest type classification. *International Journal of Remote Sensing*, 39(21), 7738–7760. <https://doi.org/10.1080/01431161.2018.1479788>
- EEA. (2018). *Copernicus land monitoring service 2018*. © European Union.
- Fayad, I., Baghdadi, N., Bazzi, H., & Zribi, M. (2020). Near real-time freeze detection over agricultural plots using Sentinel-1 data. *Remote Sensing*, 12(12), 1976. <https://doi.org/10.3390/rs12121976>
- Ford, T. W., & Quiring, S. M. (2019). Comparison of contemporary in situ, model, and satellite remote sensing soil moisture with a focus on drought monitoring. *Water Resources Research*, 55(2), 1565–1582. <https://doi.org/10.1029/2018WR024039>
- Foucras, M., Zribi, M., Albergel, C., Baghdadi, N., Calvet, J.-C., & Pellarin, T. (2020). Estimating 500-m resolution soil moisture using Sentinel-1 and optical data synergy. *Water*, 12(3), 866. <https://doi.org/10.3390/w12030866>
- Ge, Y., Thomasson, J. A., & Sui, R. (2011). Remote sensing of soil properties in precision agriculture: A review. *Frontiers of Earth Science*, 5(3), 229–238. <https://doi.org/10.1007/s11707-011-0175-0>
- Hajdu, I., Yule, I., & Dehghan-Shear, M. H. (2018). Modelling of near-surface soil moisture using machine learning and multi-temporal sentinel 1 images in New Zealand. *IGARSS 2018-2018 IEEE International Geoscience and Remote Sensing Symposium*, 1422–1425. <https://doi.org/10.1109/IGARSS.2018.8518657>
- Hegazi, E. H., Yang, L., & Huang, J. (2021). A convolutional neural network algorithm for soil moisture prediction from sentinel-1 SAR images. *Remote Sensing*, 13(24), 4964. <https://doi.org/10.3390/rs13244964>
- Hornacek, M., Wagner, W., Sabel, D., Truong, H.-L., Snoeij, P., Hahmann, T., Diedrich, E., & Doubkova, M. (2012). Potential for high resolution systematic global surface soil moisture retrieval via change detection using sentinel-1. *IEEE Journal of Selected Topics in Applied Earth Observations and Remote Sensing*, 5(4), 1303–1311. <https://doi.org/10.1109/JSTARS.2012.2190136>
- Karthikeyan, L., Pan, M., Wanders, N., Kumar, D. N., & Wood, E. F. (2017). Four decades of microwave satellite soil moisture observations: Part 1. A review of retrieval algorithms. *Advances in Water Resources*, 109, 106–120. <https://doi.org/10.1016/j.advwatres.2017.09.006>
- Kim, S., Zhang, R., Pham, H., & Sharma, A. (2019). A review of satellite-derived soil moisture and its usage for flood estimation. *Remote Sensing in Earth Systems Sciences*, 2(4), 225–246. <https://doi.org/10.1007/s41976-019-00025-7>
- Laiolo, P., Gabellani, S., Campo, L., Silvestro, F., Delogu, F., Rudari, R., Pulvirenti, L., Boni, G., Fascetti, F., Pierdicca, N., Crapolicchio, R., Hasenauer, S., & Puca, S. (2016). Impact of different satellite soil moisture products on the predictions of a continuous distributed hydrological model. *International Journal of Applied Earth Observation and Geoinformation*, 48, 131–145. <https://doi.org/10.1016/j.jag.2015.06.002>
- Lal, P., Singh, G., Das, N. N., Entekhabi, D., Lohman, R., Colliander, A., Pandey, D. K., & Setia, R. K. (2023). A multi-scale algorithm for the NISAR mission high-resolution soil moisture product. *Remote Sensing of Environment*, 295, 113667. <https://doi.org/10.1016/j.rse.2023.113667>
- Madelon, R., Rodríguez-Fernández, N. J., Bazzi, H., Baghdadi, N., Albergel, C., Dorigo, W., & Zribi, M. (2023). Soil moisture estimates at 1 km resolution making a synergistic use of Sentinel data. *Hydrology and Earth System Sciences*, 27(6), 1221–1242. <https://doi.org/10.5194/hess-27-1221-2023>
- Ma, C., Li, X., & McCabe, M. F. (2020). Retrieval of high-resolution soil moisture through combination of sentinel-1 and sentinel-2 data. *Remote Sensing*, 12(14), 2303. <https://doi.org/10.3390/rs12142303>
- Mengen, D., Jagdhuber, T., Balenzano, A., Mattia, F., Vereecken, H., & Montzka, C. (2023). High spatial and temporal soil moisture retrieval in agricultural areas using multi-orbit and vegetation adapted sentinel-1 SAR time series. *Remote Sensing*, 15(9), 2282. <https://doi.org/10.3390/rs15092282>
- Morrison, K., & Wagner, W. (2020). Explaining anomalies in SAR and scatterometer soil moisture retrievals from dry soils with subsurface scattering. *IEEE Transactions on Geoscience and Remote Sensing*, 58(3), 2190–2197. <https://doi.org/10.1109/TGRS.2019.2954771>
- Muñoz-Sabater, J., Dutra, E., Agustí-Panareda, A., Albergel, C., Arduini, G., Balsamo, G., Boussetta, S., Choulga, M., Harrigan, S., Hersbach, H., Martens, B.,

- Miralles, D. G., Piles, M., Rodríguez-Fernández, N. J., Zsoter, E., Buontempo, C., Thépaut, J.-N., others. (2021). ERA5-land: A state-of-the-art global reanalysis dataset for land applications. *Earth System Science Data*, 13(9), 4349–4383. <https://doi.org/10.5194/essd-13-4349-2021>
- Nativel, S., Ayari, E., Rodriguez-Fernandez, N., Baghdadi, N., Madelon, R., Albergel, C., & Zribi, M. (2022). Hybrid methodology using sentinel-1/sentinel-2 for soil moisture estimation. *Remote Sensing*, 14(10), 2434. <https://doi.org/10.3390/rs14102434>
- Nguyen, H. H., Cho, S., Jeong, J., & Choi, M. (2021). A D-vine copula quantile regression approach for soil moisture retrieval from dual polarimetric SAR Sentinel-1 over vegetated terrains. *Remote Sensing of Environment*, 255, 112283. <https://doi.org/10.1016/j.rse.2021.112283>
- Pathe, C., Wagner, W., Sabel, D., Doubkova, M., & Basara, J. B. (2009). Using ENVISAT ASAR global mode data for surface soil moisture retrieval over Oklahoma, USA. *IEEE Transactions on Geoscience and Remote Sensing*, 47(2), 468–480. <https://doi.org/10.1109/TGRS.2008.2004711>
- Peng, J., Albergel, C., Balenzano, A., Brocca, L., Cartus, O., Cosh, M. H., Crow, W. T., Dabrowska-Zielinska, K., Dadson, S., Davidson, M. W. J., de Rosnay, P., Dorigo, W., Gruber, A., Hagemann, S., Hirschi, M., Kerr, Y. H., Lovergine, F., Mahecha, M. D., Marzahn, P., ... Loew, A. (2020). A roadmap for high-resolution satellite soil moisture applications – confronting product characteristics with user requirements. *Remote Sensing of Environment*, 252, 112162. <https://doi.org/10.1016/j.rse.2020.112162>
- Quast, R., Wagner, W., Bauer-Marschallinger, B., & Vreugdenhil, M. (2023). Soil moisture retrieval from sentinel-1 using a first-order radiative transfer model—A case-study over the po-valley. *Remote Sensing of Environment*, 295, 113651. <https://doi.org/10.1016/j.rse.2023.113651>
- Robock, A., Vinnikov, K. Y., Srinivasan, G., Entin, J. K., Hollinger, S. E., Speranskaya, N. A., Liu, S., & Namkhai, A. (2000). The global soil moisture data bank. *Bulletin of the American Meteorological Society*, 81(6), 1281–1299. [https://doi.org/10.1175/1520-0477\(2000\)081<1281:TGSMDB>2.3.CO;2](https://doi.org/10.1175/1520-0477(2000)081<1281:TGSMDB>2.3.CO;2)
- Rüetschi, M., Schaepman, M. E., & Small, D. (2017). Using multitemporal sentinel-1 c-band backscatter to monitor phenology and classify deciduous and coniferous forests in northern switzerland. *Remote Sensing*, 10(1), 55. <https://doi.org/10.3390/rs10010055>
- Sannier, C., & Pennec, A. (2017). *GMES Initial Operations/ Copernicus Land Monitoring Services-Validation of Products -Comparative Validation of HRL-TCD and University of Maryland Global Forest Change Products.* (p. 23). <https://land.copernicus.eu/user-corner/technical-library/comparative-validation>
- Seneviratne, S. I., Corti, T., Davin, E. L., Hirschi, M., Jaeger, E. B., Lehner, I., Orlowsky, B., & Teuling, A. J. (2010). Investigating soil moisture-climate interactions in a changing climate: A review. *Earth Science Review*, 99(3–4), 125–161. <https://doi.org/10.1016/j.earscirev.2010.02.004>
- Torres, R., Snoeij, P., Geudtner, D., Bibby, D., Davidson, M., Attema, E., Potin, P., Rommen, B. Ö., Floury, N., Brown, M., Traver, I. N., Deghaye, P., Duesmann, B., Rosich, B., Miranda, N., Bruno, C., L'Abbate, M., Croci, R., Pietropaolo, A., ... Rostan, F. (2012). GMES sentinel-1 mission. *Remote Sensing of Environment*, 120, 9–24. <https://doi.org/10.1016/j.rse.2011.05.028>
- Ulaby, F.T., Richard, K. Moore, & Adrian, K. Fung. (1986). *Microwave remote sensing active and passive-volume [III]: From theory to applications.* Artech house.
- Vreugdenhil, M., Greimeister-Pfeil, I., Preimesberger, W., Camici, S., Dorigo, W., Enenkel, M., van der Schalie, R., Steele-Dunne, S., & Wagner, W. (2022). Microwave remote sensing for agricultural drought monitoring: Recent developments and challenges. *Frontiers in Water*, 4, 1045451. <https://doi.org/10.3389/frwa.2022.1045451>
- Wagner, W., Lemoine, G., & Rott, H. (1999). A method for estimating soil moisture from ERS scatterometer and soil data. *Remote Sensing of Environment*, 70(2), 191–207. [https://doi.org/10.1016/S0034-4257\(99\)00036-X](https://doi.org/10.1016/S0034-4257(99)00036-X)
- Wagner, W., Lindorfer, R., Melzer, T., Hahn, S., Bauer-Marschallinger, B., Morrison, K., Calvet, J.-C., Hobbs, S., Quast, R., Greimeister-Pfeil, I., Vreugdenhil, M., others. (2022). Widespread occurrence of anomalous C-band backscatter signals in arid environments caused by subsurface scattering. *Remote Sensing of Environment*, 276, 113025. <https://doi.org/10.1016/j.rse.2022.113025>
- Yuan, X., Ma, Z., Pan, M., & Shi, C. (2015). Microwave remote sensing of short-term droughts during crop growing seasons. *Geophysical Research Letters*, 42(11), 4394–4401. <https://doi.org/10.1002/2015GL064125>
- Zanaga, D., Van de Kerchove, R., Daems, D., De Keersmaecker, W., Brockmann, C., Kirches, G., Wevers, J., Cartus, O., Santoro, M., Fritz, S., Lesiv, M., Herold, M., Tsendbazar, N.-E., Xu, P., Ramoino, F., & Arino, O. (2022). ESA WorldCover 10 m 2021 v200.
- Zhu, L., Si, R., Shen, X., & Walker, J. P. (2022). An advanced change detection method for time-series soil moisture retrieval from sentinel-1. *Remote Sensing of Environment*, 279, 113137. <https://doi.org/10.1016/j.rse.2022.113137>